Nonlinear Ensemble Parameter Perturbation for Climate Models

XUDONG YIN

State Key Laboratory of Numerical Modeling for Atmospheric Sciences and Geophysical Fluid Dynamics (LASG), Institute of Atmospheric Physics, Chinese Academy of Sciences, and University of Chinese Academy of Sciences, Beijing, China

JUANJUAN LIU

State Key Laboratory of Numerical Modeling for Atmospheric Sciences and Geophysical Fluid Dynamics (LASG), Institute of Atmospheric Physics, Chinese Academy of Sciences, Beijing, China

BIN WANG

State Key Laboratory of Numerical Modeling for Atmospheric Sciences and Geophysical Fluid Dynamics (LASG), Institute of Atmospheric Physics, Chinese Academy of Sciences, and Center for Earth System Science, Tsinghua University, Beijing, China

(Manuscript received 30 March 2014, in final form 23 October 2014)

ABSTRACT

Model parameters can introduce significant uncertainties in climate simulations. Sensitivity analysis provides a way to quantify such uncertainties. Existing sensitivity analysis methods, however, cannot estimate the maximum sensitivity of the simulated climate to perturbations in multiple parameters. This study proposes the concept of nonlinear ensemble parameter perturbation (NEPP), which is independent of model initial conditions, to estimate the maximum effect of parameter perturbations on simulating Earth's climate. The NEPP is obtained by solving a maximization problem, whose cost function is defined by the maximum deviation of a unique ensemble of short-term predictions with large enough members caused by parameter perturbations and whose optimal solution is obtained by an ensemble-based gradient approach. This method is used to investigate the effects of NEPP on the climate of the Lorenz-63 model and a complex climate model, the Grid-Point Atmospheric Model of IAP LASG, version 2 (GAMIL2). It is found that the NEPP is capable of estimating the maximum change in climate simulation caused by perturbations in multiple parameters when the Lorenz-63 model is used. With a low computational cost, the NEPP can cause remarkable changes in the climatology of GAMIL2. The results also illustrate that the effects of parameter perturbations on short-term weather predictions and those on long-term climate simulations are correlated.

1. Introduction

There are various empirical parameters in climate models, and these parameters have great uncertainties, which may lead to significant uncertainties in climate simulations. There are many studies that quantify uncertainties in climate simulations due to uncertainties in model parameters (Webster and Sokolov 1998; Murphy et al. 2004; Stainforth et al. 2005; Tebaldi et al. 2005; Jackson et al. 2008; Meinshausen et al. 2009; Rogelj et al. 2012). Moolenaar and Selten (2004) noted that an important issue in the context of climate simulation is to identify which combination of parameter perturbations changes the simulated climate most. Since an exact simulation of the actual climate is impossible, it is of great importance to estimate the variation range of the simulated climate given the ranges of uncertainties in model parameters: in other words, to identify a particular combination of parameter perturbations, which satisfies certain constraints and is capable of causing the maximum change in climate simulation.

An exhaustive attack method would have the ability to find such an optimal combination of parameter

Corresponding author address: Juanjuan Liu, Institute of Atmospheric Physics, Chinese Academy of Sciences, P.O. Box 9804, Beijing 100029, China.
E-mail: ljjxgg@mail.iap.ac.cn

DOI: 10.1175/JCLI-D-14-00244.1

perturbations, but generally no one can afford the tremendous amount of calculations involved because it requires that massive amounts of random perturbations are superimposed on the default parameters and equal numbers of climate simulations are conducted. In addition, the adjoint method (Hall et al. 1982; Hall 1986; Janisková and Morcrette 2005; Daescu and Todling 2010) may be of some use to this issue because of the capability of computing the sensitivity of the model output to infinitesimal perturbations in all model parameters simultaneously. However, this method can only be used to obtain model sensitivity to parameters when the time scales of model predictions are not long so that the linearization assumption between parameter perturbations and the corresponding changes in model predictions is valid ("short-term prediction sensitivities"). It will collapse when computing sensitivities of long-term averaged quantities to parameters ("long-term climate sensitivities") in chaotic models (Blonigan and Wang 2014). This is because adjoint results will diverge exponentially from the true climate sensitivities because of cumulative error growth when the adjoint method is applied to trajectories that are long relative to the predictability time scales of the system (Lea et al. 2000).

Many studies have focused on the issue that sensitivities based on short-term integrations can be used for estimating the changes in the simulation of climate (e.g., Corti and Palmer 1997). Regarding the Lorenz-63 model as a climate metaphor, Lea et al. (2000) proposed an ensemble adjoint approach, in which a long integration was split into many intermediate length segments; they performed an adjoint calculation on each segment, and then averaged the results as a rough estimate of climate sensitivity (independent of initial conditions). Lea et al. (2002) applied the ensemble adjoint approach to sensitivity analyses of a chaotic ocean circulation model and stated that an unfeasibly large ensemble is required to obtain a reasonable estimate of climate sensitivity. Moolenaar and Selten (2004) attempted to find effective parameter perturbations based on the ensemble adjoint approach and illustrated that, for specific initial conditions, the parameter perturbations that cause the largest changes in the short-term integrations tend to be effective in changing the long-term climate. However, these methods are incapable of giving an estimate of the maximum change in climate simulations caused by parameter uncertainties. Moolenaar and Selten (2004) also suggested that just simply averaging optimal perturbations of short-term predictions will not necessarily yield an effective parameter perturbation for model climate. Further considerations are needed on whether the maximum change in climate simulations caused by parameter perturbations could be calculated.

In this study, we propose the concept of nonlinear ensemble parameter perturbation (NEPP), which is inspired by the conditional nonlinear optimal perturbation approach (Mu et al. 2003, 2010). The NEPP is a type of parameter perturbation independent of model initial conditions and is the most sensitive parameter perturbation for climate models, when the ensemble number of short-term predictions is large enough. This study investigates the effects of NEPP on the climate of the Lorenz-63 model (Lorenz 1963) and an atmospheric general circulation model (Li et al. 2013a), respectively. From the perspective of verifying the NEPP method, only a single model variable is considered for all numerical experiments in this study. In the next section, we define the NEPP. The impacts of NEPP on the climate of both models are presented in sections 3 and 4, respectively. Summary and discussion are given in section 5.

2. Nonlinear ensemble parameter perturbation

Let $\mathbf{M}_t(\mathbf{P})$ be the propagator of the nonlinear prediction model $\mathbf{M}$ and $\mathbf{U}_t$ be the time-dependent model state vector that is a solution to the nonlinear prediction model $\mathbf{U}_t = \mathbf{M}_t(\mathbf{P})(\mathbf{U}_0)$, where $\mathbf{P}$ is the background parameter vector and $\mathbf{U}_0$ is the initial condition.

Assuming that a parameter perturbation $\mathbf{p}'$ be superimposed on $\mathbf{P}$, the corresponding prediction deviation $\mathbf{u}_t(\mathbf{p}')$ at the prediction time t satisfies the following nonlinear relationship:

$$\mathbf{u}_t(\mathbf{p}') = \mathbf{M}_t(\mathbf{P}+\mathbf{p}')(\mathbf{U}_0) - \mathbf{M}_t(\mathbf{P})(\mathbf{U}_0). \tag{1}$$

Let us consider an ensemble including N members (each member denotes a short-term time series prediction and its time length is τ). Then, each time series prediction can be expressed as follows [suppose there are n prediction times $(t_1, t_2, \ldots, t_n)$ within a time series prediction from $t = 0$ to τ]:

$$\begin{aligned}\mathbf{y}_i &= (\mathbf{U}_{t_1}^{i\mathrm{T}}, \mathbf{U}_{t_2}^{i\mathrm{T}}, \ldots, \mathbf{U}_{t_n}^{i\mathrm{T}})^{\mathrm{T}} \\ &= \mathbf{M}_{0\to\tau}(\mathbf{P})(\mathbf{U}_0^i), \quad (i = 1, 2, \ldots, N),\end{aligned} \tag{2}$$

where the superscript T denotes the transpose of a vector, $\mathbf{M}_{0\to\tau}$ denotes a continuous time series prediction including the model states corresponding to all prediction times within $[0, \tau]$, and $\mathbf{U}_0^i$ is the initial condition of the ith time series prediction. The deviation from each time series prediction caused by p' can be expressed as follows:

$$\begin{aligned}\mathbf{y}_i'(\mathbf{p}') = (\mathbf{u}_{t_1}^{i\mathrm{T}}, \mathbf{u}_{t_2}^{i\mathrm{T}}, \ldots, \mathbf{u}_{t_n}^{i\mathrm{T}})^{\mathrm{T}} &= \mathbf{M}_{0\to\tau}(\mathbf{P}+\mathbf{p}')(\mathbf{U}_0^i) \\ &- \mathbf{M}_{0\to\tau}(\mathbf{P})(\mathbf{U}_0^i), \quad (i = 1, 2, \ldots, N).\end{aligned} \tag{3}$$

We then introduce the definition of NEPP, a parameter perturbation that maximizes the cost function, which is an ensemble average of the square of the L_2 norm of the short-term time series prediction deviation over the model attractor. More specifically, a parameter perturbation $\mathbf{p}'^*$ is called the NEPP if and only if

$$J(\mathbf{p}'^*) = \max_{\mathbf{p}' \in C_\delta} J(\mathbf{p}'), \tag{4}$$

where

$$J(\mathbf{p}') = \frac{1}{N}\sum_{i=1}^{N} \|\mathbf{M}_{0\to\tau}(\mathbf{P}+\mathbf{p}')(\mathbf{U}_0^i) - \mathbf{M}_{0\to\tau}(\mathbf{P})(\mathbf{U}_0^i)\|_2^2. \tag{5}$$

In Eq. (5), $\|\ \|_2$ denotes the L_2 norm, $\mathbf{p}' \in C_\delta$ is a constraint, and C_δ is a closed set. The constraint can be simply expressed as belonging to a sphere with a specific norm. Of course, we can also investigate the condition that the parameter perturbations satisfy some physical laws. The variable N denotes the ensemble number, and the length of each time series prediction (τ) can be referred to as the time scale of the NEPP.

Assume that the independent random variables X_1, X_2, ..., X_n have the following probability distribution:

$$f(x) = \begin{cases} p(x), & 0 \le x \le a \\ 0, & x < 0 \quad \text{or} \quad x > a \end{cases}, \tag{6}$$

where a is a positive number and $p(x)$ is a continuous function defined over the interval of $[0, a]$. The mathematical expectation of the independent random variables follows that

$$E(X_i) = \int_0^a x p(x)\, dx = c, \tag{7}$$

where c is a constant depending on $p(x)$. Using the Khinchine's weak law of large numbers (Rose and Smith 2002), we can obtain

$$Z_n = \frac{1}{n}\sum_{i=1}^{n} X_n \xrightarrow{P} c, \quad (n \to \infty), \tag{8}$$

where $\xrightarrow{P}$ P denotes the convergence in probability.

Assuming that the initial points of all the ensemble members are selected with an equal probability over the attractor of a chaotic model, $\mathbf{U}_0^i$ (for $i = 1, 2, \ldots, N$) would satisfy a uniform distribution over the attractor; therefore, for a specific parameter perturbation $\mathbf{p}'$, $J_i(\mathbf{p}') = \|\mathbf{M}_{0\to\tau}(\mathbf{P}+\mathbf{p}')(\mathbf{U}_0^i) - \mathbf{M}_{0\to\tau}(\mathbf{P})(\mathbf{U}_0^i)\|_2^2$ (for $i = 1, 2, \ldots, N$) will follow an independent, identical distribution similar to Eq. (6). In the same way, we can obtain

$$J(\mathbf{p}') = \frac{1}{N}\sum_{i=1}^{N} J_i(\mathbf{p}') \xrightarrow{P} C, \quad \text{as} \quad N \to \infty, \tag{9}$$

where C is independent of model initial conditions and depends only on the parameter perturbation $\mathbf{p}'$ and the time scale τ. Then, the NEPP satisfying Eq. (4) corresponds to the maximum value of C at a specific time scale. In a similar way, assuming that the mapping $\mathbf{p}' \to J(\mathbf{p}')$ is continuous and one to one, we can obtain

$$\mathbf{p}'^* \xrightarrow{P} \mathbf{c}_p, \quad \text{as} \quad N \to \infty, \tag{10}$$

where $\mathbf{c}_p$ is a constant vector independent of model initial conditions and depends only on the time scale.

An ideal representation of the ensemble average is to average $J_i(\mathbf{p}')$ (for $i = 1, 2, \ldots, N$) over a great number of orbits starting from different initial points $\mathbf{U}_0^i$ (for $i = 1, 2, \ldots, N$) equiprobably on the attractor of the model. In fact, the precondition that $J_i(\mathbf{p}')$ (for $i = 1, 2, \ldots, N$) follows an independent, identical distribution may not be satisfied theoretically when this method is applied to the climate system that involves high-dimensional state vectors, since the initial points of the ensemble members cannot be selected with an equal probability over the attractor of a climate model. For a long-term climate simulation whose integration time is T, as an approximation of the ensemble average, we would like to choose N ensemble members of short-term model predictions whose initial points are selected with an equal probability within $[0, T]$. This selection of ensemble members may be effective, provided that the ensemble number is large enough. In this paper, the maximization problem of Eqs. (4) and (5) is solved by an ensemble-based gradient method (Yin et al. 2014).

3. The impact of NEPP on the climate of the Lorenz-63 model

The variation in the simulated climate caused by a given parameter perturbation can be expressed as follows:

$$\begin{aligned} \Delta\overline{\mathbf{U}} &= \left\| \frac{1}{T}\int_0^T \mathbf{U}_t(\mathbf{P}+\mathbf{p}')\, dt - \frac{1}{T}\int_0^T \mathbf{U}_t(\mathbf{P})\, dt \right\|_2 \\ &= \left\| \frac{1}{T}\int_0^T \mathbf{u}_t(\mathbf{p}')\, dt \right\|_2, \end{aligned} \tag{11}$$

where T is a long model integration time and other notations are the same as those in section 2.

TABLE 1. The NEPPs satisfying the L_2-norm constraint of Eq. (15) and the corresponding cost functions with respect to an ever-increasing ensemble number N. The time scale τ is set to 0.20, and the NEPPs shown are standardized.

N	Maximum of cost function	Nonlinear ensemble parameter perturbation (σ'/σ, r'/r, b'/b)
100	75.49	$(0.6225 \times 10^{-2}, 9.809 \times 10^{-2}, -1.840 \times 10^{-2})$
500	67.17	$(0.8377 \times 10^{-2}, 9.821 \times 10^{-2}, -1.690 \times 10^{-2})$
1000	67.19	$(0.8781 \times 10^{-2}, 9.818 \times 10^{-2}, -1.685 \times 10^{-2})$
5000	66.53	$(0.8884 \times 10^{-2}, 9.818 \times 10^{-2}, -1.679 \times 10^{-2})$
10 000	66.54	$(0.8889 \times 10^{-2}, 9.817 \times 10^{-2}, -1.682 \times 10^{-2})$

To apply the principle (Hoskins 1983) that a hierarchy of numerical models is available to investigate the topics of interest, ranging from simple models to state-of-the-art models, we first consider a simple model in this section, the nonlinear dissipative Lorenz-63 system (Lorenz 1963), which is often used to mimic atmospheric chaotic behavior due to a qualitative similarity between the chaotic dynamics of the Lorenz-63 model and those of large-scale atmospheric circulation (Palmer 1993, 1999). Chu (1999) used this model to investigate model sensitivity to inaccurate initial conditions and to inaccurate parameters. Thuburn (2005) stated that the Lorenz-63 system reflects many of the relevant properties of the full climate system and that it is likely that deterministic full climate models and the Lorenz-63 model have similar complex attractors. The Lorenz-63 model has three differential equations, which are derived from the convection equations of Saltzman (1962) and whose solutions afford the simplest example of deterministic nonperiodic flow. The equations of the Lorenz-63 model are as follows:

$$\frac{dx}{dt} = \sigma(y - x),$$
$$\frac{dy}{dt} = rx - y - xz, \quad \text{and}$$
$$\frac{dz}{dt} = xy - bz, \tag{12}$$

where σ (the Prandtl number), r (a normalized Raleigh number), and b (a nondimensional wavenumber) are model parameters. The state variables x, y, and z measure the intensity of convective motion, the temperature difference between the ascending and descending flows, and the distortion of vertical temperature profile from linearity, respectively. Following Lea et al. (2000), we also focus on the variation of the climate $\overline{z}$ (the bar means average over time) caused by a parameter perturbation $\mathbf{p}'$,

$$\Delta\overline{z} = \left| \frac{1}{T}\int_0^T z_t(\mathbf{P} + \mathbf{p}')\,dt - \frac{1}{T}\int_0^T z_t(\mathbf{P})\,dt \right|, \tag{13}$$

where $T = 100$ (time units) is a very long integration time, which could be analogous to a climate integration of a general circulation model (Lea et al. 2000), and the background parameter vector is denoted by $\mathbf{P} = (\sigma, r, b)^{\mathrm{T}}$, which is set to $(10, 28, 8/3)^{\mathrm{T}}$ in this study. Here, the parameter perturbation vector is denoted by $\mathbf{p}' = (\sigma', r', b')^{\mathrm{T}}$, and the standardized parameter perturbation vector is denoted by $\boldsymbol{\alpha}' = (\alpha_1', \alpha_2', \alpha_3')^{\mathrm{T}}$, with

$$\alpha_1' = \sigma'/\sigma, \quad \alpha_2' = r'/r, \quad \text{and} \quad \alpha_3' = b'/b. \tag{14}$$

First of all, we investigate the situation that the parameter perturbations satisfy a L_2-norm constraint,

$$C_\delta = \{(\alpha_1', \alpha_2', \alpha_3') \,|\, \|\boldsymbol{\alpha}'\|_2 = \sqrt{\alpha_1'^2 + \alpha_2'^2 + \alpha_3'^2} \le \delta = 10\%\}. \tag{15}$$

The cost function of the NEPP of the Lorenz-63 model can be expressed as follows:

$$J(\mathbf{p}') = \frac{1}{N}\sum_{i=1}^{N}\int_0^\tau [z_t(\mathbf{P} + \mathbf{p}')(\mathbf{U}_0^i) - z_t(\mathbf{P})(\mathbf{U}_0^i)]^2\,dt. \tag{16}$$

Then, we evaluate the effect of the ensemble number of short-term predictions on the direction of the NEPP through a group of numerical experiments with $\tau = 0.2$ (time units). The results in Table 1 show that both the NEPP and its corresponding cost function tend to be stable asymptotically with the increase of ensemble number and remain constant when N exceeds 1000. As we noted in section 2, this result manifests that the NEPP is a constant vector independent of model initial conditions so long as the ensemble number is large enough. Hence, with an ensemble of 5000 members that is enough for the NEPP to become a stable constant vector, we obtain a series of NEPPs with respect to an increasing time scale (τ). With these NEPPs, we calculate variations in the simulated climate $\Delta\overline{z}$ according to Eq. (16). Table 2 presents the results with the time scale τ set to 0.10, 0.20, 0.30, 0.40, and 0.50 time units. One can see that the variations in the simulated climate caused by the NEPPs with $\tau \le 0.40$ are generally close to each other.

TABLE 2. The NEPPs satisfying the L_2-norm constraint of Eq. (15) with respect to different time scales τ. The ensemble number N is chosen to be 5000, and the NEPPs shown are standardized.

τ (time unit)	Nonlinear ensemble parameter perturbation (σ'/σ, r'/r, b'/b)	Variation in the climate
0.10	$(0.8102 \times 10^{-2}, 9.324 \times 10^{-2}, -3.522 \times 10^{-2})$	2.814
0.20	$(0.8884 \times 10^{-2}, 9.818 \times 10^{-2}, -1.679 \times 10^{-2})$	3.092
0.30	$(0.9158 \times 10^{-2}, 9.903 \times 10^{-2}, -1.042 \times 10^{-2})$	2.965
0.40	$(0.9372 \times 10^{-2}, 9.946 \times 10^{-2}, -0.4536 \times 10^{-2})$	2.832
0.50	$(0.8514 \times 10^{-2}, 9.962 \times 10^{-2}, 2.038 \times 10^{-2})$	2.890

To evaluate whether the NEPPs can cause maximum variation in the simulated climate, we have not yet found a better way than the exhaustive attack method: that is, 10^6 random parameter perturbations are generated, which satisfy the L_2-norm equality constraint (since the maximum of $\Delta\overline{z}$ is always reached on the boundary of the sphere $\|\boldsymbol{\alpha}'\|_2 \le \delta$ if the mapping $\boldsymbol{\alpha}' \to \Delta\overline{z}$ is continuous and one to one),

$$\|\boldsymbol{\alpha}'\|_2 = \sqrt{\alpha_1'^2 + \alpha_2'^2 + \alpha_3'^2} = \delta = 10\%, \qquad (17)$$

and the same amount of $\Delta\overline{z}$ is acquired through 10^6 integrations of the Lorenz-63 model. Figure 1 shows the distribution of the probability to select a parameter perturbation that yields $\Delta\overline{z} \ge X$: that is, $1 - \mathrm{CDF}(X)$, the cumulative distribution function (CDF) of X, which is the abscissa of Fig. 1. The small red segment in Fig. 1 represents the cumulative probabilities to select a parameter perturbation that yields $\Delta\overline{z} \ge X$ when X is greater than 2.820 000; values in the red segment are all less than 0.99%. When X is greater than 2.920 000, the cumulative probabilities are all less than 0.01% and close to zero. In particular, the variations in the simulated climate caused by the NEPPs with a successively increasing time scale from $\tau = 0.01$ to 0.50 are shown in Fig. 2 (blue curve). In order to better assess the results, we draw a red line in Fig. 2, which represents the value of $\Delta\overline{z}$ that equals 2.820 000, beyond which the corresponding cumulative probabilities are all less than 0.99%. We can see clearly that the values of $\Delta\overline{z}$ caused by NEPPs with the time scales from $\tau = 0.11$ to 0.50 are all greater than or equal to 2.820 000. Thus, from Figs. 1 and 2, we know that the values of $\Delta\overline{z}$ caused by the NEPPs with the time scales from $\tau = 0.11$ to 0.50 all correspond to a very small cumulative probability of less than 0.99%, while the NEPPs with too short time scales ($\tau \le 0.06$) can hardly yield a large variation of $\overline{z}$. This may be primarily because the model needs a finite time to display its nonlinear response to parameter perturbations: that is, for too short time scales, the sensitivity of model prediction to parameters may be too weak and can hardly provide enough information for the estimation of the maximum change in climate simulation. However, we can see in detail in Table 2 that the perturbation in the third parameter (b) changes from a negative value to a positive value as the time scale increases, which may indicate that the appropriate time scales should be less than 0.5 time units, although the NEPPs with longer time scales still yield a very large variation of $\overline{z}$ (not shown). Lea et al. (2000) also indicated that the magnitude of the initial condition–dependent effects would be too large for the ensemble of short-term predictions to uncover the underlying climate sensitivity, if

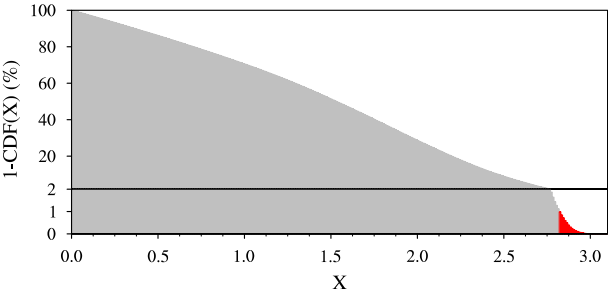

FIG. 1. Distribution of the probability to select a parameter perturbation satisfying the L_2-norm equality constraint of Eq. (17) that yields $\Delta\overline{z} \ge X$: that is, $1 - \mathrm{CDF}(X)$. Note the change of scale in the y axis. Particularly, the probabilities corresponding to the small red segment at the end are all less than or equal to the probability of 0.99%.

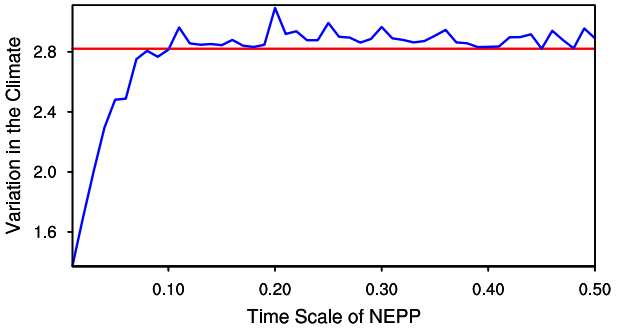

FIG. 2. Variation in the simulated climate $\overline{z}$ (the blue curve) caused by the NEPPs satisfying the L_2-norm constraint of Eq. (15) with time scales from $\tau = 0.1$ to 0.50. The red line represents a critical value that the ordinate equals 2.820 000, beyond which the cumulative probabilities belong to the red segment in Fig. 1.

TABLE 3. The NEPPs satisfying the L_∞-norm constraint of Eq. (18) with respect to different time scales τ. The ensemble number N is chosen to be 500.

τ (time unit)	Nonlinear ensemble parameter perturbation (σ', r', b')	Maximum of cost function
0.10	(1.000, 2.800, −0.2667)	11.42
0.20	(1.000, 2.800, −0.2667)	106.6
0.30	(1.000, 2.800, −0.2667)	298.9
0.40	(1.000, 2.800, −0.2667)	556.9
0.50	(1.000, 2.800, 0.2667)	981.0

TABLE 4. The local NEPPs satisfying the L_∞-norm constraint of Eq. (18) with respect to different time scales (τ). The ensemble number (N) is chosen to be 500.

τ (time unit)	Local nonlinear ensemble parameter perturbation (σ', r', b')	Local maximum of cost function
0.10	(−1.000, −2.800, 0.2667)	9.838
0.20	(−1.000, −2.800, 0.2667)	85.37
0.30	(−1.000, −2.800, 0.2667)	237.5
0.40	(−1.000, −2.800, 0.2667)	451.2
0.50	(−1.000, −2.800, −0.2667)	687.4

the time scales of short-term predictions are too long. Moreover, the time scales should also not be so long that the linearization assumption is invalid for obtaining the NEPP, which is similar to the statement of Corti and Palmer (1997). Besides, the directions of the NEPPs are consistent, especially with $\tau = 0.10$, 0.20, 0.30, and 0.40, which indicate that the NEPPs are a type of parameter perturbations belonging to the most sensitive perturbations for model climate.

Nevertheless, for general circulation models (GCMs), values of empirical parameters have their own upper and lower bounds and their errors are often not dependent on each other. Since the maximum effect of parameter errors on climate simulation is our main focus, it would be of more practical use to ensure that values of all the parameters can vary independently within their own variation range when the cost function is optimized to its maximum. Typically, the parameter space can be standardized to a L_∞-norm space, so a L_∞-norm constraint could be applied to obtain the NEPPs in this study. In view of these situations, we investigate the variations in the climate of the Lorenz-63 model caused by the NEPPs with a L_∞-norm constraint,

$$C_\delta = \{(\alpha_1', \alpha_2', \alpha_3') \mid \|\boldsymbol{\alpha}'\|_\infty \le \delta\} = \{(\sigma', r', b') \mid |\sigma'|/\sigma \le \delta, |r'|/r \le \delta, |b'|/b \le \delta\}, \quad (18)$$

where $\|\ \|_\infty$ denotes the L_∞ norm, and $\delta = 10\%$. Then, a series of NEPPs with different time scales are obtained, with 500 ensemble members of short-term predictions used. The results are shown in Table 3. We can see that the NEPPs with the time scales of $\tau = 0.10$, 0.20, 0.30, and 0.40 are all the same, while the sign of the third perturbation (b') of the NEPP ($\tau = 0.5$) is opposite to that of the NEPPs ($\tau \le 0.4$). This may indicate that the NEPP with a L_∞-norm constraint depends less on the time scale, provided that the time scale is not too long. In addition, we find that there exists a possibility that the cost function attains its local maximum in a small neighborhood of a point in the phase space, which is similar to the results of Mu and Wang (2001) and Mu et al. (2004) that showed local maxima in obtaining their optimal nonlinear initial perturbations. Mu and Wang (2001) found the local optimal perturbations resulted from the nonlinearity of the numerical model and in linear cases there exists only a global maximum but no local maximum. Likewise, the NEPP proposed in this study is a type of optimal parameter perturbation, so it is reasonable that there exist some local maxima of the cost function in this study. We refer to the perturbation corresponding to the local maximum of the cost function as local NEPP and the one corresponding to the global maximum as global NEPP accordingly. Table 4 displays a series of local NEPPs with $\tau = 0.10$, 0.20, 0.30, 0.40, and 0.50. We can observe easily that the directions of local NEPPs are opposite to those of global NEPPs; therefore, local NEPP may possess clear physical meanings in some cases.

Furthermore, we would like to evaluate whether the NEPPs with a L_∞-norm constraint can also cause maximum variation in the simulated climate. The exhaustive attack method is employed again, that is, 10^6 random parameter perturbations are generated, satisfying the L_∞-norm constraint of Eq. (18), and the same amount of $\Delta\overline{z}$ is acquired through 10^6 integrations of the Lorenz-63 model. Figure 3 shows the distribution of the probability to select a parameter perturbation with the L_∞-norm constraint of Eq. (18) that yields $\Delta\overline{z} \ge X$. In particular, whether the variation in the simulated climate caused by global NEPPs ($\tau \le 0.40$) or by local NEPPs ($\tau \le 0.40$) corresponds to cumulative probabilities less than 0.06%, which are displayed in Fig. 3 as a small red segment. Of course, the effect of global NEPP and that of local NEPP on the simulated climate are just the opposite: that is, one makes $\overline{z}$ increase maximally and the other makes $\overline{z}$ decrease maximally (not shown). In this respect, the variation range of $\overline{z}$ due to uncertainties in model parameters can also be estimated, because global NEPP and local NEPP could correspond to the upper and lower bounds of the variation range of $\overline{z}$, respectively. Besides, it is

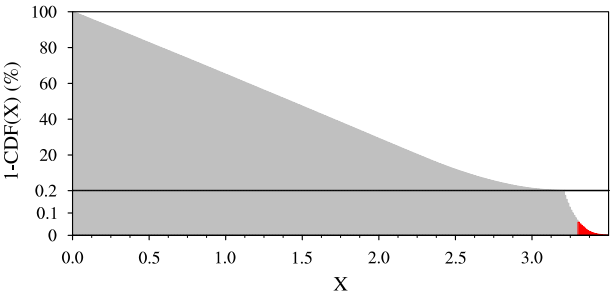

FIG. 3. Distribution of the probability to select a parameter perturbation satisfying the L_∞-norm constraint of Eq. (18) that yields $\Delta\overline{z} \geq X$. The rest of the experiment setup is the same as in Fig. 1. Particularly, the probabilities corresponding to the small red segment at the end are all less than or equal to the probability of 0.06%.

found that both global NEPP and local NEPP for the time scale equal to 0.5 time units cannot exert a large influence on the simulated climate, which indicates once more that the appropriate time scales of the NEPP should be less than 0.5 time units and thus is consistent with the results when a L_2-norm constraint is adopted.

4. The impact of NEPP on the climate of GAMIL2

To assess the impact of NEPP on the climate of a more realistic model, we use a complex climate model, the Grid-Point Atmospheric Model of IAP LASG, version 2 (GAMIL2; Li et al. 2013a). GAMIL2 is an atmospheric general circulation model (AGCM) based on a finite difference dynamical core, which was developed by the State Key Laboratory for Numerical Modeling of Atmospheric Sciences and Geophysical Fluid Dynamics (LASG) at the Institute of Atmospheric Physics (IAP) under the Chinese Academy of Sciences (CAS), and an atmospheric component model of the CMIP5 model FGOALS-g2 (Li et al. 2013b). GAMIL2 has a horizontal resolution of 2.8° × 2.8° and 26 levels. The dynamical core of GAMIL2 is a gridpoint framework developed by Wang et al. (2004) that ensures mass conservation and the effective total energy conservation under the standard stratification approximation. This dynamical core is computationally highly stable without any filtering or smoothing in the polar region, on account of the use of a weighted equal-area grid in the high latitudes (Wang et al. 2004). GAMIL2 employs the deep convective parameterization scheme by Zhang and Mu (2005), the convective cloud fraction scheme by Xu and Krueger (1991), and the cloud microphysical scheme by Morrison and Gettelman (2008). For more detail about GAMIL2, readers are referred to Li et al. (2013a). In this study, a parallel version of GAMIL2 with 2D parallel decomposition (Liu et al., 2014a) is used for faster computing speed. All simulations related to GAMIL2 are conducted on the Community Coupler (C-Coupler) platform (Liu et al. 2014b), with the C-Coupler platform providing the functionality for configuring, compiling and running the simulations.

Arakawa (2004) noted that cumulus convection plays a central role in most of the interactions between various processes in the climate system and is a key process for producing precipitation and redistributing atmospheric heat and moisture; therefore, cumulus parameterization is at the core of numerically modeling the atmosphere. However, Dai (2006) found that most of the AGCMs can hardly reproduce the observed magnitude of convective versus stratiform precipitation ratio by the Tropical Rainfall Measuring Mission (TRMM) Precipitation Radar data. TRMM data showed that around 40% of the total tropical precipitation was from stratiform precipitation (Schumacher and Houze 2003). As in most AGCMs, the partitioning between the convective and stratiform precipitation in GAMIL2 is also biased, while the total precipitation is reasonably simulated (Li et al. 2013a).

Over these years, the effects of different parameter combinations on model behavior of interest have been explored by many studies. Murphy et al. (2004) investigated the variation range of climate simulations consistent with parameter uncertainties by perturbing 29 parameters controlling key physical characteristics of subgrid-scale atmospheric and surface processes. Subsequently, Stainforth et al. (2005) selected six parameters affecting the representation of clouds and precipitation from the parameters explored by Murphy et al. (2004) and discovered a wider range of possible responses of the climate system by creating an ensemble of ensembles in which an initial condition ensemble is used for each combination of perturbed parameters. Knight et al. (2007) present an extremely large ensemble of climate model runs in which 10 parameters, initial conditions, and the hardware and software have all been varied and demonstrated that 80% of variation in model response to carbon dioxide is associated with variation in a small subset of parameters mostly concerned with cloud dynamics. Following these studies, we selected three parameters, the rain water autoconversion coefficient (c0), the evaporation efficiency (ke), and the threshold value for cape (capelmt), which all belong to the deep convection parameterization scheme of GAMIL2 and may play an important role in affecting the convective precipitation process. Then the joint effects of the three parameters on the simulated climatology (30 yr, from 1970 to 1999) of convective versus total precipitation ratio of GAMIL2 are investigated using the NEPP method. Unlike Murphy et al. (2004) presenting the uncertainty

TABLE 5. Detailed information about uncertain parameters chosen in the deep convection parameterization scheme of GAMIL2.

Parameter	Description	Default value	Range
c0	Rain water autoconversion coefficient for deep convection	5.0×10^{-4}	2.5×10^{-4} to 7.5×10^{-4}
ke	Evaporation efficiency for deep convection	9.0×10^{-6}	4.5×10^{-6} to 13.5×10^{-6}
capelmt	Threshold value for cape for deep convection	80.0	40.0 to 120.0

ranges of 32 surface and atmospheric variables estimated by a perturbed physics ensemble, this study just focused on a single model output, because the objective of this study is to test and verify the effectiveness of the NEPP method. If uncertainties of multiple model outputs are intended to be considered, the cost function [Eq. (5)] can be extended to include multiple model outputs and then maximized in a similar way as the case of single model output.

Detailed information about these parameters is shown in Table 5, where the ranges of parameter values are chosen to be much smaller than their realistic ranges and are symmetric around their default values for simplicity. Here, the background parameter vector is denoted by $\mathbf{P} = (P_{c0}, P_{ke}, P_{capelmt})^T$, which is set to its default value, and the parameter perturbation vector is denoted by $\mathbf{p}' = (p'_{c0}, p'_{ke}, p'_{capelmt})^T$. Thereby, the constraint of the parameter perturbations can be set to a L_∞-norm sphere,

$$C_\delta = \{(p'_{c0}, p'_{ke}, p'_{capelmt}) | |p'_{c0}|/P_{c0} \le \delta, |p'_{ke}|/P_{ke} \le \delta, |p'_{capelmt}|/P_{capelmt} \le \delta\}, \tag{19}$$

where $\delta = 50\%$ and the ranges of parameter perturbations are consistent with those of the three parameters. Of course, in realistic cases, ranges of uncertain parameters could be different and asymmetric around their default values, and then the constraints of parameter perturbations need to be specified according to actual requirements.

The convective versus total precipitation ratio is defined by

$$R = \frac{\text{Convective precipitation rate}}{\text{Total (convective and large-scale) precipitation rate}}, \tag{20}$$

and the global vector of R is denoted by $\mathbf{R}$ accordingly. First, a long integration of GAMIL2 with default parameters is performed from 1 January 1969 to 31 December 1999, where the first year is discarded as model spinup. Then the initial points of all the ensemble members of short-term time series predictions are selected uniformly from this default integration of GAMIL2 between 1 January 1970 and 31 December 1999. Then different time scales (τ = 12, 24, and 48 h) of short-term time series predictions of 3-h-average $\mathbf{R}$ are used to calculate the NEPPs. That means there are 4, 8, and 16 predictions of 3-h-average $\mathbf{R}$ within each short-term time series prediction, respectively. Let $\mathbf{R}^{3h}$ denote a global vector of 3-h-average $\mathbf{R}$. Then, the cost function of the NEPP of GAMIL2 can be expressed as follows:

$$J(\mathbf{p}') = \frac{1}{N}\sum_{i=1}^{N}\int_0^\tau \|\mathbf{R}_t^{3h}(\mathbf{P}+\mathbf{p}')(\mathbf{U}_0^i) - \mathbf{R}_t^{3h}(\mathbf{P})(\mathbf{U}_0^i)\|_2^2\, dt, \tag{21}$$

where the ensemble number N adopted here is 720. The NEPPs with different time scales (τ = 12, 24, and 48 h) all converge to same parameter perturbations, which are shown in Table 6 and marked with an asterisk. The corresponding maximum cost function values are 195.8, 774.0, and 2921.3, respectively. The global vector of the 30-yr climatology of $\mathbf{R}$ is denoted by $\overline{\mathbf{R}}$ and its deviation vector is denoted by $\Delta\overline{\mathbf{R}}$. The variation in the climate of GAMIL2 caused by a parameter perturbation $\mathbf{p}'$ is expressed as the root-mean-square of $\Delta\overline{\mathbf{R}}$,

$$\text{rms}(\Delta\overline{\mathbf{R}}) = \sqrt{\frac{1}{n_{grid}}\|\Delta\overline{\mathbf{R}}\|_2^2} = \sqrt{\frac{1}{n_{grid}}\|\overline{\mathbf{R}}(\mathbf{P}+\mathbf{p}') - \overline{\mathbf{R}}(\mathbf{P})\|_2^2}, \tag{22}$$

where $n_{grid} = 128 \times 60$ is the total horizontal grid number of GAMIL2.

First of all, the default climatology (45°S–45°N) of convective versus total precipitation ratio of GAMIL2 with default parameters and the perturbed climatology of

TABLE 6. The individual parameter perturbations and a chosen parameter perturbation combination in which only the sign of p'_{ke} is opposite to that of the NEPP.

Parameter perturbations $(p'_{c0}, p'_{ke}, p'_{capelmt})$	Variation in the 30-yr climate
$(-2.5 \times 10^{-4}, 4.5 \times 10^{-6}, -40.0)$*	2.951×10^{-2}
$(-2.5 \times 10^{-4}, 0.0, 0.0)$	2.115×10^{-2}
$(0.0, 4.5 \times 10^{-6}, 0.0)$	1.056×10^{-2}
$(0.0, 0.0, -40.0)$	0.518×10^{-2}
$(-2.5 \times 10^{-4}, -4.5 \times 10^{-6}, -40.0)$	1.492×10^{-2}

* The variation in the climate of GAMIL2 caused by the NEPP.

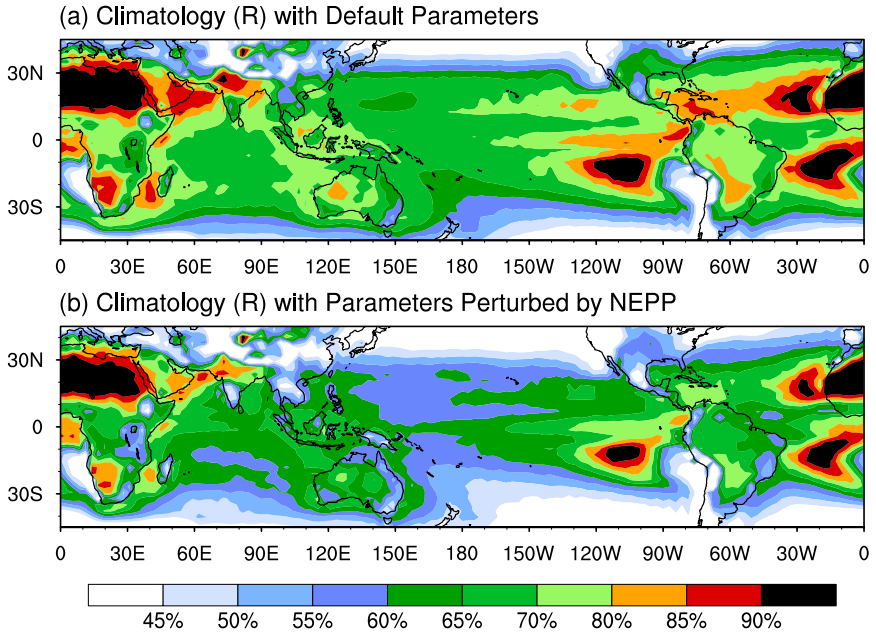

FIG. 4. (a) The default 30-yr climatology of convective vs total precipitation ratio R of GAMIL2 with default parameters and (b) the perturbed 30-yr climatology of GAMIL2 with parameters perturbed by the NEPP.

GAMIL2 with parameters perturbed by the NEPP are shown in Fig. 4. We can observe that the climatology of **R** is reduced significantly in most regions, which indicates that the climatology of **R** is sensitive to the NEPP on the whole. For better comparison, some individual parameter perturbation experiments are conducted; three of the experiments are shown in Table 6, and another three have smaller effects on the simulated climate (not shown). From Table 6, we find that the NEPP gives rise to a much larger rms($\Delta\overline{\mathbf{R}}$) than any individual parameter perturbation, which manifests that the NEPP is an effective combination of parameter perturbations capable of yielding a very large effect on $\overline{\mathbf{R}}$, although it cannot be completely certain whether the NEPP has indeed produced the largest impact on climate simulation because of the incapability to afford to employ the exhaustive attack method to verify this point.

In particular, the variations in the 30-yr climatology (45°S–45°N) of **R** caused by the NEPP and the three individual parameter perturbations are shown in Fig. 5. We can observe clearly that the variations in $\overline{\mathbf{R}}$ caused by the latter two individual parameter perturbations ($p'_{\mathrm{ke}} = 4.5 \times 10^{-6}$ and $p'_{\mathrm{capelmt}} = -40.0$) overall fall between −4% and 4% throughout the field (45°S–45°N), while the first individual parameter perturbation ($p'_{\mathrm{c0}} = -2.5 \times 10^{-4}$) causes larger changes in the climatology of **R**. So, we may assume that the first individual parameter perturbation plays a leading role in affecting the climatology of **R**. The latter two individual parameter perturbation can only exert small influences on $\overline{\mathbf{R}}$, while the second individual parameter perturbation has a slightly larger effect than the third one. Moreover, Fig. 5 shows that the first individual parameter perturbation has a large reduction effect on the climatology of **R** in most regions, except for the Peru coast and the tropical Atlantic. By contrast, the NEPP ($p'_{\mathrm{c0}} = -2.5 \times 10^{-4}$, $p'_{\mathrm{ke}} = 4.5 \times 10^{-6}$, and $p'_{\mathrm{capelmt}} = -40.0$) yields a much more remarkable change in the climatology, in which a larger and broader reduction of $\overline{\mathbf{R}}$ is obtained, and the increasing effects of the first individual parameter perturbation on $\overline{\mathbf{R}}$ over the Peru coast and the tropical Atlantic decrease significantly and even disappear. The impact of NEPP on the climatology may be a kind of nonlinearly combined effects of the three perturbations, where the effects of $p'_{\mathrm{ke}} = 4.5 \times 10^{-6}$ and $p'_{\mathrm{capelmt}} = -40.0$ largely strengthen the reduction effect of $p'_{\mathrm{c0}} = -2.5 \times 10^{-4}$ on the climatology of **R**.

In order to illustrate that the variation in the simulated climate caused by different perturbations in the three parameters may be counteracted by each other to a certain extent, another parameter perturbation combination ($p'_{\mathrm{c0}} = -2.5 \times 10^{-4}$, $p'_{\mathrm{ke}} = -4.5 \times 10^{-6}$, and $p'_{\mathrm{capelmt}} = -40.0$), in which only the sign of $p'_{\mathrm{ke}} = -4.5 \times 10^{-6}$ is opposite to that of the NEPP, is superimposed on the background parameter vector **P**. It is shown in Table 6 that rms($\Delta\overline{\mathbf{R}}$) caused by this perturbation is much smaller than that caused by the NEPP and even that caused by the individual parameter perturbation ($p'_{\mathrm{c0}} = -2.5 \times 10^{-4}$),

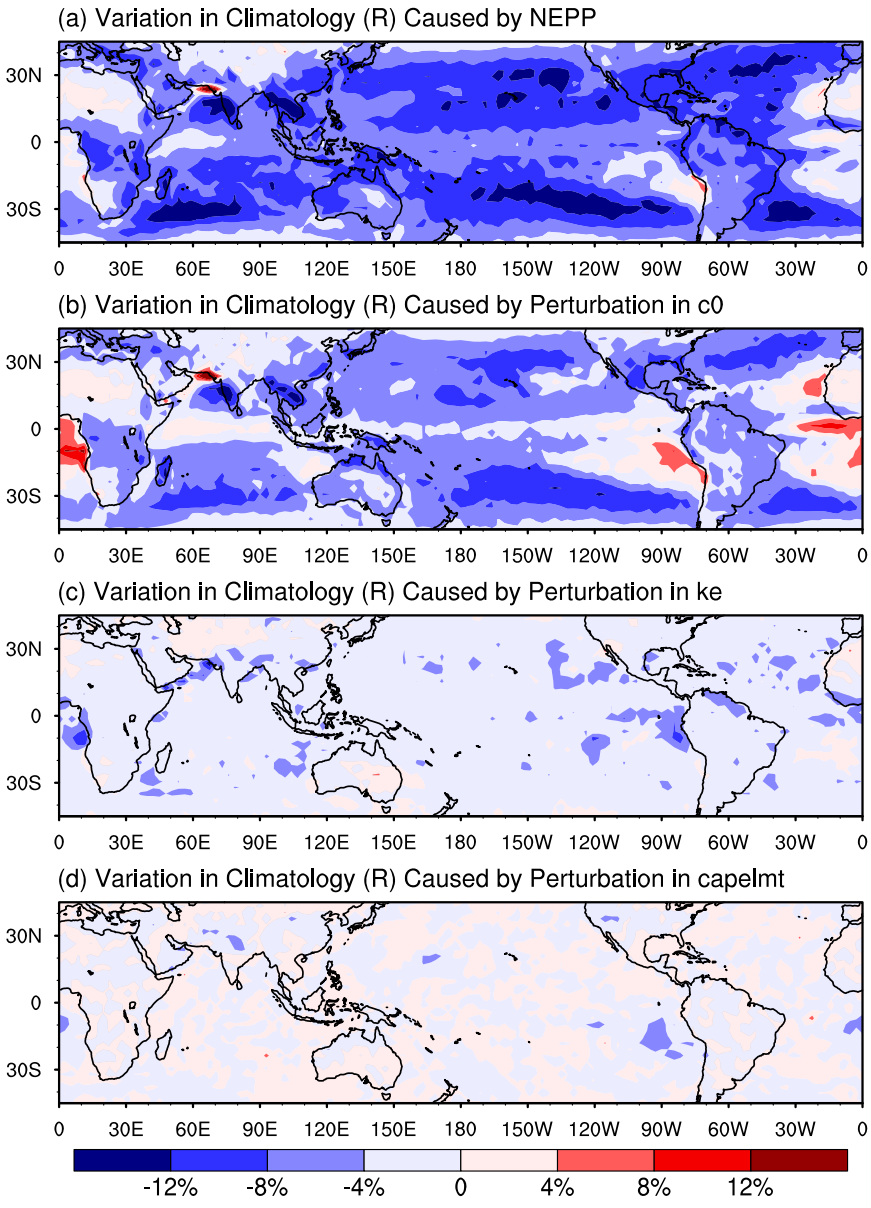

FIG. 5. The variations in the 30-yr climatology of convective vs total precipitation ratio of GAMIL2 caused by (a) the NEPP (-2.5×10^{-4}, 4.5×10^{-6}, -40.0), (b) the first individual parameter perturbation (-2.5×10^{-4}, 0, 0), (c) the second individual parameter perturbation (0, 4.5×10^{-6}, 0), and (d) the third individual parameter perturbation (0, 0, -40.0).

which indicates that a negative perturbation ($p'_{ke} = -4.5 \times 10^{-6}$) would counteract the reduction effect of the parameter perturbation ($p'_{c0} = -2.5 \times 10^{-4}$) on $\overline{\mathbf{R}}$ and thus weaken the change in the simulated climate. Furthermore, the time series variations in the annual mean convective versus total precipitation ratio from the year of 1970 to 1999 caused by the NEPP (-2.5×10^{-4}, 4.5×10^{-6}, -40.0), the first individual parameter perturbation (-2.5×10^{-4}, 0, 0), the second individual parameter perturbation (0, 4.5×10^{-6}, 0), the third individual parameter perturbation (0, 0, -40.0), and the parameter perturbation combination (-2.5×10^{-4}, -4.5×10^{-6}, -40.0), in which only the sign of p'_{ke} is opposite to that of the NEPP, are shown in different colors in Fig. 6. Similarly, the variations from 1970 to 1999 caused by the NEPP are all much larger than other parameter perturbations. Since the perturbation ($p'_{ke} = -4.5 \times 10^{-6}$) could counteract the reduction effect of the perturbation ($p'_{c0} = -2.5 \times 10^{-4}$) on the annual mean convective versus total precipitation ratio, the time series variations caused by the parameter perturbation combination (-2.5×10^{-4}, -4.5×10^{-6},

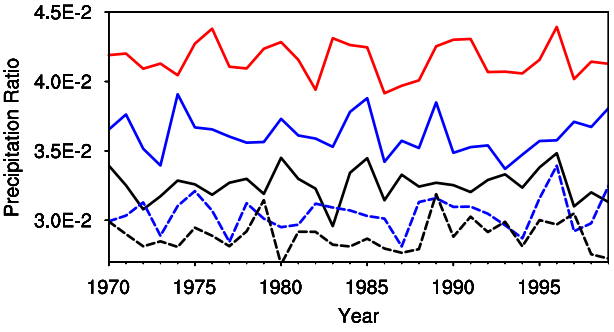

FIG. 6. The time series variations in the annual mean convective vs total precipitation ratio of GAMIL2 from 1970 to 1999 caused by the NEPP (-2.5×10^{-4}, 4.5×10^{-6}, -40.0) (red curve), the first individual parameter perturbation (-2.5×10^{-4}, 0, 0) (blue curve), the second individual parameter perturbation (0, 4.5×10^{-6}, 0) (blue dashed curve), the third individual parameter perturbation (0, 0, -40.0) (black dashed curve), and a chosen parameter perturbation combination (-2.5×10^{-4}, -4.5×10^{-6}, -40.0) (black curve) in which only the sign of p'_{ke} is opposite to that of the NEPP.

-40.0) are also less than the first individual parameter perturbation (-2.5×10^{-4}, 0, 0). Thus, these results are consistent with those in Table 6 and also indicate that the NEPP is capable of causing significant changes in climate simulation.

Besides, the computational cost of the NEPP method is relatively low. This is because the convergence rate of the NEPP is generally fast: that is, the optimization procedure to maximize the cost function of Eq. (21) could converge after three iterations in this case. Assuming that the number of iterations is denoted by n_{iter} and the number of parameters is denoted by n_p, the total model integration time needed to obtain the NEPP is generally $(n_{\mathrm{iter}} + n_p)N\tau$. Thus, the model integration time needed to obtain the NEPP with respect to $\tau = 48$ model hours in this case is 8640 model days (approximately 24 model years) and even less than the model integration time of a 30-yr climate simulation. Finally, it must be declared that the issue how the NEPP affects the climatology of convective versus total precipitation ratio simulated by GAMIL2 from the perspective of physical mechanism is beyond scope of this study and is a subject of our future investigation.

5. Summary and discussion

Previous studies on climate sensitivities (Corti and Palmer 1997; Lea et al. 2000, 2002; Eyink et al. 2004; Moolenaar and Selten 2004) showed that short-term integrations could be used for investigating long-term climate sensitivities, but existing methods are still incapable of giving an estimate of the maximum sensitivity of the simulated climate to perturbations in model parameters. In this study, we propose a novel method to cope with this problem, which seeks a type of parameter perturbation (named the NEPP) under a given constraint that maximizes the deviation of a unique ensemble of short-term predictions with large enough members. An ensemble-based gradient approach is employed to obtain the optimal solution of this maximization problem. The NEPP is demonstrated to be independent of model initial conditions both theoretically and experimentally. First of all, using the Lorenz-63 model as a proxy for climate chaotic behavior, we illustrated that the NEPPs satisfying the L_2-norm constraint and the L_∞-norm constraint are capable of yielding maximum variations in the simulated climate, through a series of numerical experiments. In the case of the L_∞-norm constraint, the concept of local NEPP is introduced. Local NEPP corresponds to the local maximum of the cost function, and its direction is generally opposite to that of global NEPP. It is expected that the variation range of the simulated climate due to uncertainties in model parameters can be estimated by means of both global NEPP and local NEPP.

The method, then, is used to investigate the effects of NEPP on the climate of GAMIL2, which is an AGCM. In this case, we pay attention to the variations in the 30-yr climatology of convective versus total precipitation ratio caused by the NEPP of three uncertain parameters in the deep convection parameterization scheme of GAMIL2. It is found that the NEPP is capable of giving rise to remarkable changes in the climatology of GAMIL2, while the NEPP can be obtained at a relatively low computational cost. Since we could not afford to employ the exhaustive attack method, which needs tremendous amount of climate simulations, some individual parameter perturbation experiments are conducted instead to verify the NEPP method. The results show that the climatology with respect to parameters perturbed by the NEPP is reduced significantly in most regions compared with the default climatology, and the NEPP causes a much larger change in the 30-yr climate than any individual parameter perturbation. In addition, for atmospheric models, most perturbations to initial conditions are rather ineffective, so most parameter perturbations are bound to be ineffective for similar reasons (Moolenaar and Selten 2004), which indicates that there are a relatively low number of unstable directions of parameter perturbations. In this regards, it is certain that the NEPP could represent an effective parameter perturbation combination and belong to a type of sensitive parameter perturbation for climate models.

As for the reason why the NEPP could cause maximum variation in the simulated climate theoretically, we may attribute it to a close correlation between the cost function [Eq. (5)] proposed in this study and the

variation in the simulated climate [Eq. (11)]: both of which are independent of model initial conditions. As a large ensemble number of short-term integrations over the attractor may reflect climatological characteristics of the model, the sensitivity of this ensemble of short-term predictions to parameter perturbations is likely to be consistent with that of a long-term average of model trajectories. The results in this study illustrate that the effects of parameter perturbations on short-term weather predictions and those on long-term climate simulations are correlated. This is consistent with the indication of Orrell (2003) that there is a link between short-term predictability and long-term predictability, and studies of short-term model error may likewise yield information on the effects of model errors for climate studies. Moreover, from the perspective of physical mechanism, Hoskins (2013) also noted that the verification and improvement of short-term predictions, which are important in their feedbacks onto longer time scales, could provide support for long-term predictions.

In fact, previous studies (Murphy et al. 2004; Stainforth et al. 2005; Barnett et al. 2006; Knight et al. 2007) that focus on the quantification of model uncertainties associated with parameters also attempted to estimate the ranges of uncertainties in climate change projections, by running a perturbed physics ensemble in which model parameters are set to different plausible values. This perturbed parameter approach had proved valuable in addressing uncertainties in climate simulations (Slingo and Palmer 2011). This approach is capable of finding a distribution of climate simulations, while the NEPP method cannot make it. However, the generation of the perturbed physics ensemble may be a challenge to general computational resources, while the climateprediction.net project using idle processing capacity on personal computers volunteered by members of the public can afford it (Knight et al. 2007). Moreover, as Stainforth et al. (2005) suggested, many of the parameter combinations explored have relatively little effect on model behavior, which may be because multiple perturbations may have mutually compensating effects when averaged on global scales. In this respect, the NEPP method that attempts to obtain effective parameter perturbation combinations may be of some use to quantify the uncertainty range of climate simulation. In addition, some other studies (Jackson et al. 2008; Villagran et al. 2008; Jackson 2009) attempt to reduce model uncertainties by calibrating parameters in GCMs based on a set of observed data. These studies are capable of estimating a posterior joint probability distribution for uncertain parameters by means of Bayesian inference, which can identify the sources of uncertainty and select the appropriate combination of parameter values (Jackson 2009). Jackson (2009) also stated that Bayesian inference assumes all parameter choices are correlated and the number of parameter samples needed to quantify these correlations is very large, so the number of parameters explored in this framework is limited. The NEPP method proposed in this study may provide useful information to identify the most sensitive parameter combinations for Bayesian inference, because this method could determine the maximum effect of perturbations in multiple parameters on climate models at a relatively low cost; that is, the larger the effect of selected parameters on model behavior is, the more sensitive the parameter choices are. Besides, since the objective of this study is to test and verify the effectiveness of the NEPP method, this study focused only on a single model output, while some other studies like Murphy et al. (2004) paid attention to the uncertainty ranges of multiple model variables estimated by a perturbed physics ensemble. If uncertainties of multiple model outputs are intended to be considered, the cost function [Eq. (5)] can be extended to include all these model outputs and then maximized in a similar way as the case of single model output. Of course, the NEPP with respect to multiple model outputs may be different from that with respect to single model output and needed to be explored in the future.

Finally, we consider that the limited range of time scales for all the individual ensemble members of short-term predictions may be a key limitation to apply this method to investigate the maximum effect of parameter perturbations on climate simulation. Since the valid range of time scales is usually estimated by experience or some information associated with the predictability time scales of atmospheric or oceanic motions, the NEPP method may fail to obtain the most effective parameter perturbation if the time scale adopted is beyond its valid range. In addition, as it is widely admitted that the oceanic motions are much slower that the atmospheric motions, the time scales of the NEPP method suitable for ocean general circulation models (OGCMs) may be much longer than those suitable for AGCMs, which means that 48 h used in this study may be too short for OGCMs. To cope with this problem, different time scales of the individual ensemble members can be tested in advance when the NEPP method is applied to investigate the impact of parameter errors on OGCMs. In this way, the valid range of time scales could be estimated roughly by comparing the results. Since the NEPP maximizes the ensemble average of nonlinear variation of short-term integrations and could exert a nonlinear effect on climate simulation, it is expected that the NEPP should have the ability to yield an approximate maximum change in climate simulation even for high-dimensional climate models, if appropriate short-term predictions are considered. These issues would

require future investigation, but the result presented in this study that the NEPP obtained at a relatively low computational cost can cause great changes in the climate of GAMIL2 is encouraging.

Acknowledgements. The authors would like to thank four anonymous reviewers for their constructive suggestions. This study is jointly supported by the Ministry of Science and Technology of China (for funding the 973 Project through Grant 2010CB951604), the National Science and Technology Support Program (Grant 2012BAC22B02), and the National Natural Science Foundation of China (Grant 41105120).

REFERENCES

Arakawa, A., 2004: The cumulus parameterization problem: Past, present, and future. *J. Climate,* **17,** 2493–2525, doi:10.1175/1520-0442(2004)017<2493:RATCPP>2.0.CO;2.

Barnett, D. N., S. J. Brown, J. M. Murphy, D. M. H. Sexton, and M. J. Webb, 2006: Quantifying uncertainty in changes in extreme event frequency in response to doubled CO_2 using a large ensemble of GCM simulations. *Climate Dyn.,* **26,** 489–511, doi:10.1007/s00382-005-0097-1.

Blonigan, P. J., and Q. Wang, 2014: Probability density adjoint for sensitivity analysis of the mean of chaos. *J. Comput. Phys.,* **270,** 660–686, doi:10.1016/j.jcp.2014.04.027.

Chu, P. C., 1999: Two kinds of predictability in the Lorenz system. *J. Atmos. Sci.,* **56,** 1427–1432, doi:10.1175/1520-0469(1999)056<1427:TKOPIT>2.0.CO;2.

Corti, S., and T. N. Palmer, 1997: Sensitivity analysis of atmospheric low-frequency variability. *Quart. J. Roy. Meteor. Soc.,* **123,** 2425–2447, doi:10.1002/qj.49712354413.

Daescu, D. N., and R. Todling, 2010: Adjoint sensitivity of the model forecast to data assimilation system error covariance parameters. *Quart. J. Roy. Meteor. Soc.,* **136,** 2000–2012, doi:10.1002/qj.693.

Dai, A., 2006: Precipitation characteristics in eighteen coupled climate models. *J. Climate,* **19,** 4605–4630, doi:10.1175/JCLI3884.1.

Eyink, G. L., T. W. N. Haine, and D. J. Lea, 2004: Ruelle's linear response formula, ensemble adjoint schemes and Lévy flights. *Nonlinearity,* **17,** 1867–1889, doi:10.1088/0951-7715/17/5/016.

Hall, M. C., 1986: Application of adjoint sensitivity theory to an atmospheric general circulation model. *J. Atmos. Sci.,* **43,** 2644–2651, doi:10.1175/1520-0469(1986)043<2644:AOASTT>2.0.CO;2.

——, D. G. Cacuci, and M. E. Schlesinger, 1982: Sensitivity analysis of a radiative-convective model by the adjoint method. *J. Atmos. Sci.,* **39,** 2038–2050, doi:10.1175/1520-0469(1982)039<2038:SAOARC>2.0.CO;2.

Hoskins, B. J., 1983: Dynamical processes in the atmosphere and the use of models. *Quart. J. Roy. Meteor. Soc.,* **109,** 1–21, doi:10.1002/qj.49710945902.

——, 2013: The potential for skill across the range of the seamless weather-climate prediction problem: A stimulus for our science. *Quart. J. Roy. Meteor. Soc.,* **139,** 573–584, doi:10.1002/qj.1991.

Jackson, C. S., 2009: Use of Bayesian inference and data to improve simulations of multi-physics climate phenomena. *J. Phys.,* **180,** 012029, doi:1742-6596/180/1/012029.

——, M. K. Sen, G. Huerta, Y. Deng, and K. P. Bowman, 2008: Error reduction and convergence in climate prediction. *J. Climate,* **21,** 6698–6709, doi:10.1175/2008JCLI2112.1.

Janisková, M., and J. J. Morcrette, 2005: Investigation of the sensitivity of the ECMWF radiation scheme to input parameters using the adjoint technique. *Quart. J. Roy. Meteor. Soc.,* **131,** 1975–1995, doi:10.1256/qj.04.183.

Knight, C. G., and Coauthors, 2007: Association of parameter, software, and hardware variation with large-scale behavior across 57,000 climate models. *Proc. Natl. Acad. Sci. USA,* **104,** 12 259–12 264, doi:10.1073/pnas.0608144104.

Lea, D. J., M. R. Allen, and T. W. Haine, 2000: Sensitivity analysis of the climate of a chaotic system. *Tellus,* **52,** 523–532, doi:10.1034/j.1600-0870.2000.01137.x.

——, T. W. Haine, M. R. Allen, and J. A. Hansen, 2002: Sensitivity analysis of the climate of a chaotic ocean circulation model. *Quart. J. Roy. Meteor. Soc.,* **128,** 2587–2605, doi:10.1256/qj.01.180.

Li, L., and Coauthors, 2013a: Evaluation of Grid-point Atmospheric Model of IAP LASG version 2 (GAMIL2). *Adv. Atmos. Sci.,* **30,** 855–867, doi:10.1007/s00376-013-2157-5.

——, and Coauthors, 2013b: The Flexible Global Ocean-Atmosphere-Land System model, grid-point version 2: FGOALS-g2. *Adv. Atmos. Sci.,* **30,** 543–560, doi:10.1007/s00376-012-2140-6.

Liu, L., R. Li, G. Yang, B. Wang, L. Li, and Y. Pu, 2014a: Improving parallel performance of a finite-difference AGCM on modern high-performance computers. *J. Atmos. Oceanic Technol.,* **31,** 2157–2168, doi:10.1175/JTECH-D-13-00067.1.

——, G. Yang, B. Wang, C. Zhang, R. Li, Z. Zhang, Y. Ji, and L. Wang, 2014b: C-Coupler1: A Chinese community coupler for Earth system modelling. *Geosci. Model Dev.,* **7,** 2281–2302, doi:10.5194/gmd-7-2281-2014.

Lorenz, E. N., 1963: Deterministic nonperiodic flow. *J. Atmos. Sci.,* **20,** 130–141, doi:10.1175/1520-0469(1963)020<0130:DNF>2.0.CO;2.

Meinshausen, M., N. Meinshausen, W. Hare, S. C. Raper, K. Frieler, R. Knutti, D. J. Frame, and M. R. Allen, 2009: Greenhouse-gas emission targets for limiting global warming to 2°C. *Nature,* **458,** 1158–1162, doi:10.1038/nature08017.

Moolenaar, H. E., and F. M. Selten, 2004: Finding the effective parameter perturbations in atmospheric models: The LORENZ63 model as case study. *Tellus,* **56A,** 47–55, doi:10.1111/j.1600-0870.2004.00043.x.

Morrison, H., and A. Gettelman, 2008: A new two-moment bulk stratiform cloud microphysics scheme in the Community Atmosphere Model, version 3 (CAM3). Part I: Description and numerical tests. *J. Climate,* **21,** 3642–3659, doi:10.1175/2008JCLI2105.1.

Mu, M., and J. Wang, 2001: Nonlinear fastest growing perturbation and the first kind of predictability. *Sci. China,* **44,** 1128–1139, doi:10.1007/BF02906869.

——, W. Duan, and B. Wang, 2003: Conditional nonlinear optimal perturbation and its applications. *Nonlinear Processes Geophys.,* **10,** 493–501, doi:10.5194/npg-10-493-2003.

——, L. Sun, and H. A. Dijkstra, 2004: The sensitivity and stability of the ocean's thermohaline circulation to finite amplitude perturbations. *J. Phys. Oceanogr.,* **34,** 2305–2315, doi:10.1175/1520-0485(2004)034<2305:TSASOT>2.0.CO;2.

——, W. Duan, Q. Wang, and R. Zhang, 2010: An extension of conditional nonlinear optimal perturbation approach and its applications. *Nonlinear Processes Geophys.,* **17,** 211–220, doi:10.5194/npg-17-211-2010.

Murphy, J. M., D. M. Sexton, D. N. Barnett, G. S. Jones, M. J. Webb, M. Collins, and D. A. Stainforth, 2004: Quantifying

uncertainties in climate change from a large ensemble of general circulation model predictions. *Nature,* **430,** 768–772, doi:10.1038/nature02771.

Orrell, D., 2003: Model error and predictability over different timescales in the Lorenz '96 systems. *J. Atmos. Sci.,* **60,** 2219–2228, doi:10.1175/1520-0469(2003)060<2219:MEAPOD>2.0.CO;2.

Palmer, T. N., 1993: Extended-range atmospheric prediction and the Lorenz model. *Bull. Amer. Meteor. Soc.,* **74,** 49–65, doi:10.1175/1520-0477(1993)074<0049:ERAPAT>2.0.CO;2.

——, 1999: A nonlinear dynamical perspective on climate prediction. *J. Climate,* **12,** 575–591, doi:10.1175/1520-0442(1999)012<0575:ANDPOC>2.0.CO;2.

Rogelj, J., M. Meinshausen, and R. Knutti, 2012: Global warming under old and new scenarios using IPCC climate sensitivity range estimates. *Nat. Climate Change,* **2,** 248–253, doi:10.1038/nclimate1385.

Rose, C., and M. D. Smith, 2002: *Mathematical Statistics with Mathematica.* Springer-Verlag, 311 pp.

Saltzman, B., 1962: Finite amplitude free convection as an initial value problem—I. *J. Atmos. Sci.,* **19,** 329–341, doi:10.1175/1520-0469(1962)019<0329:FAFCAA>2.0.CO;2.

Schumacher, C., and R. A. Houze, 2003: Stratiform rain in the tropics as seen by the TRMM Precipitation Radar. *J. Climate,* **16,** 1739–1756, doi:10.1175/1520-0442(2003)016<1739:SRITTA>2.0.CO;2.

Slingo, J., and T. Palmer, 2011: Uncertainty in weather and climate prediction. *Philos. Trans. Roy. Soc. London,* **A369,** 4751–4767, doi:10.1098/rsta.2011.0161.

Stainforth, D. A., and Coauthors, 2005: Uncertainty in predictions of the climate response to rising levels of greenhouse gases. *Nature,* **433,** 403–406, doi:10.1038/nature03301.

Tebaldi, C., R. L. Smith, D. Nychka, and L. O. Mearns, 2005: Quantifying uncertainty in projections of regional climate change: A Bayesian approach to the analysis of multimodel ensembles. *J. Climate,* **18,** 1524–1540, doi:10.1175/JCLI3363.1.

Thuburn, J., 2005: Climate sensitivities via a Fokker–Planck adjoint approach. *Quart. J. Roy. Meteor. Soc.,* **131,** 73–92, doi:10.1256/qj.04.46.

Villagran, A., G. Huerta, C. S. Jackson, and M. K. Sen, 2008: Computational methods for parameter estimation in climate models. *Bayesian Anal.,* **3,** 823–850, doi:10.1214/08-BA331.

Wang, B., H. Wan, Z. Ji, X. Zhang, R. Yu, Y. Yu, and H. Liu, 2004: Design of a new dynamical core for global atmospheric models based on some efficient numerical methods. *Sci. China,* **47,** 4–21, doi:10.1360/04za0001.

Webster, M. D., and A. Sokolov, 1998: Quantifying the uncertainty in climate predictions. MIT Joint Program on the Science and Policy of Global Change Rep. 37, 23 pp. [Available online at http://hdl.handle.net/1721.1/3610.]

Xu, K. M., and S. K. Krueger, 1991: Evaluation of cloudiness parameterizations using a cumulus ensemble model. *Mon. Wea. Rev.,* **119,** 342–367, doi:10.1175/1520-0493(1991)119<0342:EOCPUA>2.0.CO;2.

Yin, X., B. Wang, J. Liu, and X. Tan, 2014: Evaluation of conditional nonlinear optimal perturbation obtained by an ensemble-based approach using the Lorenz-63 model. *Tellus,* **66A,** 22773, doi:10.3402/tellusa.v66.22773.

Zhang, G. J., and M. Mu, 2005: Effects of modifications to the Zhang-McFarlane convection parameterization on the simulation of the tropical precipitation in the National Center for Atmospheric Research Community Climate Model, version 3. *J. Geophys. Res.,* **110,** D09109, doi:10.1029/2004JD005617.